

# An In-Frame Deletion in the NS Protein-Coding Sequence of Parvovirus H-1PV Efficiently Stimulates Export and Infectivity of Progeny Virions

Nadine Weiss, Alexandra Stroh-Dege, Jean Rommelaere, Christiane Dinsart, and Nathalie Salomé

Program Infection and Cancer, Division Tumor Virology F010, and Institut National de la Santé et de la Recherche Médicale U701, Deutsches Krebsforschungszentrum, Heidelberg, Germany

An in-frame, 114-nucleotide-long deletion that affects the NS-coding sequence was created in the infectious molecular clone of the standard parvovirus H-1PV, thereby generating Del H-1PV. The plasmid was transfected and further propagated in permissive human cell lines in order to analyze the effects of the deletion on virus fitness. Our results show key benefits of this deletion, as Del H-1PV proved to exhibit (i) higher infectivity (lower particle-to-infectivity ratio) *in vitro* and (ii) enhanced tumor growth suppression *in vivo* compared to wild-type H-1PV. This increased infectivity correlated with an accelerated egress of Del H-1PV progeny virions in producer cells and with an overall stimulation of the viral life cycle in subsequently infected cells. Indeed, virus adsorption and internalization were significantly improved with Del H-1PV, which may account for the earlier appearance of viral DNA replicative forms that was observed with Del H-1PV than wild-type H-1PV. We hypothesize that the internal deletion within the NS2 and/or NS1 protein expressed by Del H-1PV results in the stimulation of some step(s) of the viral life cycle, in particular, a maturation step(s), leading to more efficient nuclear export of infectious viral particles and increased fitness of the virus produced.

Rodent parvoviruses (PVs), including the rat parvovirus H-1PV, belong to the genus *Parvovirus* within the subfamily *Parvovirinae*, whose members are endogenous to vertebrates. These autonomous parvoviruses are small, nonenveloped viruses and display an icosahedral capsid in which a single-stranded DNA genome of about 5,000 nucleotides is packaged (17). The parvoviral genome mainly consists of two large overlapping open reading frames under the control of two promoters (11, 17). The early promoter, P4, drives the expression of the viral nonstructural proteins NS1 and NS2 (18, 48), while the late promoter, P38, controls the expression of the viral capsid proteins VP1 and VP2 and of the nonstructural protein SAT (48, 54). NS1 is a multifunctional, mainly nuclear, phosphorylated protein of about 83 kDa that is required for the replication of the viral genome, in particular, due to its helicase, endonuclease, ATPase, and site-specific DNA-binding activities (15, 30). Besides its function in viral DNA replication, NS1 transactivates the P38 promoter (10, 20, 30), plays a critical role in the vesicular egress of progeny virions (1, 38), and is the main determinant of parvoviral cytotoxicity (30, 39). Like NS1, the small NS2 proteins (about 25 kDa) are essential for various steps of the parvovirus life cycle, but unlike NS1, they do not appear to display any enzymatic activity. The NS2 proteins of the parvovirus minute virus of mice, prototype strain (MVMp), consist of three isoforms that are generated by alternative splicing and differ in their carboxyl termini (14). Although NS2 has been reported to play a role during viral DNA replication (9, 15, 36), translation of viral mRNA (28, 29, 37), capsid assembly (12), and parvoviral cytotoxicity (6, 8), the specific NS2 function(s) is still unclear. Both phosphorylated and nonphosphorylated forms of NS2 exist, and these are mainly located in the cytoplasm. However, nonphosphorylated NS2 can also be detected in the nuclei of infected cells (14). NS2 was shown to interact with at least two members of the 14-3-3 protein family (7) and with the survival motor neuron (SMN) protein (52, 53). In addition, all three iso-

forms of NS2 shuttle from the nucleus to the cytoplasm by interacting with the nuclear export factor CRM1 (5, 41). A supraphysiological nuclear export signal (supraNES) was recently identified in NS2 and is involved in the interaction of NS2 with CRM1 and in the cytoplasmic sequestration of CRM1, which accumulates at the nuclear periphery in infected cells (22). Efficient nuclear export of MVMp virions in mouse fibroblasts is also dependent on NS2. Consistently, viruses with a mutated NS2 NES fail to be exported to the cytoplasm and display dramatically reduced fitness in culture, supporting a critical role of CRM1/NS2 interaction in the control of the maturation and egress of viral particles (21, 34).

Our laboratory previously isolated a naturally occurring fully infectious variant of H-1PV, designated H-1 dr virus, which was able to supplant the standard H-1PV strain in coinfecting newborn human kidney cell line NB-E (23). H-1 dr virus exhibits an in-frame deletion in the open reading frame encoding the nonstructural proteins NS1 and NS2 and a duplication of a 58-nucleotide repeated sequence inboard from the right-hand palindrome (23). The 114-nucleotide-long deletion in the H-1 dr genome results in shortened NS1 and NS2 proteins, in agreement with their molecular mass reduction. However, besides a greater accumulation of NS2-encoding R2 transcripts and higher levels of neosynthesized NS2 proteins, no significant differences between H-1 dr and H-1 standard viruses were detected with regard to their ability to produce viral DNA replicative forms (RFs), progeny single-stranded DNA, or capsids (23). Both nonstructural proteins are also known


Received 26 January 2012 Accepted 23 April 2012

Published ahead of print 2 May 2012

Address correspondence to Nathalie Salomé, n.salome@dkfz.de.

Copyright © 2012, American Society for Microbiology. All Rights Reserved.

doi:10.1128/JVI.00212-12

to play  roles at late steps of the virus life cycle, such as the formation of progeny viral particles and their intracellular trafficking from the nucleus to the plasma membrane of infected cells (1, 12, 38). This prompted us to further analyze the effects of the above-mentioned in-frame deletion within the nonstructural genes on the production and egress of progeny virus in the absence of the sequence duplication found in the right-hand hairpin of the H-1 dr genome. To this end, the deletion was introduced in an infectious molecular clone of the standard H-1PV genome, generating the plasmid pDelH1. Our results show key benefits of the deletion for progeny virions produced from Del H-1PV (compared with wild-type [wt] H-1PV) regarding (i) the release and particle-to-infectivity (P/I) ratio *in vitro* and (ii) their ability to suppress tumor growth *in vivo*. We hypothesize that the shortened NS2 and/or NS1 products expressed by Del H-1PV are more efficient than the corresponding full-length proteins in driving some step(s) of the viral life cycle, in particular, a maturation step(s) leading to nuclear export of infectious viral particles and overall fitness of the virus produced.

## MATERIALS AND METHODS

**Plasmid construct.** The infectious molecular clone of wild-type H-1PV, designated pH1, has been described previously (24). The deletion in the NS-coding sequence of the H-1PV genome (i.e., deletion of nucleotides [nt] 2022 to 2135) was introduced into pH1 by cloning a 557-bp ApoI-HindIII PCR DNA fragment which contains the 114-bp deleted region generated with the help of the forward primer 5'-CTATAAATTCGCTA GGTCAATGCGCTCACCATCTCTGACTCCGAGCCAAAACACTGG GGAGGCTGGTTCC-3' and reverse primer 5'-GAAAGCTTAGGTGCA AAAGCTCGCTTGG-3'. This resulted in the pDelH1 plasmid construct in which the substituted ApoI-HindIII fragment was further verified by sequencing (GATC Biotech, Constance, Germany).

**Cell cultures.** Simian virus 40 (SV40)-transformed human newborn kidney NB-324K cells (49) were propagated in Eagle's minimal essential medium (MEM; Sigma-Aldrich) supplemented with 5% fetal bovine serum (FBS; PAA Laboratories, Pasching, Austria), 2 mM L-glutamine (Invitrogen), and antibiotics (100 U/ml of penicillin G and 100 µg/ml of streptomycin sulfate; Invitrogen).

Human pancreatic ductal adenocarcinoma (PDAC) cell lines Panc-1 and MiaPaCa-2 were kindly provided by A. Vecchi (Istituto Clinico Humanitas, Rozzano, Italy). The human cervix carcinoma cell line HeLa was kindly provided by E. Schwarz (DKFZ, Heidelberg, Germany). The simian virus 40 T antigen-, adenovirus type 5-transformed human cell line 293T/17 (43) was obtained from the American Type Culture Collection (Manassas, VA). Panc-1, MiaPaCa-2, HeLa, and 293T/17 cells were grown in Dulbecco's modified Eagle's medium (DMEM; Sigma-Aldrich) supplemented with 10% FBS, 2 mM L-glutamine, and antibiotics (100 U/ml of penicillin G and 100 µg/ml of streptomycin sulfate).

**Transfection assays.** Transfections of 293T cells were performed using the CaPO<sub>4</sub> precipitation method. Briefly, 6 µg of pH1 or pDelH1 plasmid DNA was precipitated in a mixture of a HEPES-buffered saline solution and a calcium chloride (CaCl<sub>2</sub>) solution as described elsewhere (24, 27). After incubation at room temperature for 20 min, the DNA-containing mixture was added dropwise to the culture medium of  $2 \times 10^6$  293T cells, which were then incubated at 37°C in 5% CO<sub>2</sub>.

Transfections of NB-324K cells were performed using Lipofectamine 2000 (Invitrogen). Briefly, at 30 to 60 min prior to transfection, complete cell culture medium was exchanged by fresh medium without supplements. Six micrograms of pH1 or pDelH1 plasmid DNA was diluted in Opti-MEM (Invitrogen), and the mixture was added to a Lipofectamine 2000 solution according to the manufacturer's instructions. After incubation at room temperature for 25 min, the mixture was added dropwise to the cell culture medium of subconfluent NB-324K cells. At 4 h posttrans-

fection (p.t.), the medium was replaced by fresh, complete cell culture medium.

For virus production, cells were harvested at 2 to 3 days posttransfection and cell-bound virus particles were extracted as described below.

**Virus infection and production.** The Del H-1PV mutant and wt H-1PV were primarily produced by transfection of 293T cells with appropriate plasmid constructs as described above and subsequently amplified by infection of NB-324K cells at a multiplicity of infection (MOI) of  $3 \times 10^{-3}$  PFU/cell. Upon appearance of cytopathic effects in most of the cell population, i.e., at 2 to 3 days postinfection (p.i.), cells were harvested and lysed in VTE buffer (50 mM Tris, pH 8.7, 0.5 mM EDTA) by means of three freeze-thaw cycles. Cell debris was removed by centrifugation, and virus stocks were purified by iodixanol step gradient centrifugation (55) and further titrated as described below.

For the kinetics analysis of virus production,  $1 \times 10^5$  cells were infected with Del H-1PV or wt H-1PV at an MOI of 0.5 PFU/cell. At various times postinfection, medium was collected and infected cell culture was harvested and subjected to three freeze-thaw cycles in VTE buffer. Virus titers were determined for both the cell extract and the culture medium by plaque assay.

**Titration of infectious and full particles.** Infectious viral particles were titrated by plaque assay or by hybridization assays on NB-324K indicator cells as previously described (27, 49). Virus titers were expressed as numbers of PFU or replication units (RU) per milliliter of virus suspension.

Full viral particles were quantified either by dot blot hybridization assays or by quantitative real-time PCR as described previously (24, 26). Virus titers were expressed as the number of viral genomes (vg) per milliliter of virus suspension.

**Analysis of plaque size.** To determine the size of plaques and their occurrence frequency, plaque assays were performed as described elsewhere (49) with minor modifications. Briefly,  $1.4 \times 10^6$  NB-324K cells were seeded on a 10-cm cell culture dish (Sarstedt, Nürnbrecht, Germany) and infected with either wt H-1PV at an MOI of 0.05 vg/cell or Del H-1PV at an MOI of 0.0125 vg/cell. After infection, 20 ml of overlay medium was added to each dish, and at 6 days postinfection, living cells were stained with 8 ml/dish of neutral red-containing staining solution. The number and size of the plaques were measured using the Java-based image-processing software ImageJ (National Institutes of Health).

**Measurement of tumor suppression *in vivo*.** Cultures of Panc-1 cells were infected *in vitro* with either Del H-1PV or wild-type H-1PV at an MOI of 1 RU/cell and implanted subcutaneously (s.c.) into the right flank of BALB/c nude mice. At 4 h postinfection, groups of 6 or 7 mice were injected with 200 µl of cell suspension ( $5 \times 10^6$  cells/mouse) containing either mock-treated (i.e., buffer-treated) or wt H-1PV- or Del H-1PV-infected Panc-1 cells. Treated mice (6- to 7-week-old females, four animals per cage) were maintained in isolators at 21 to 24°C with 40 to 60% humidity. Tumor sizes were measured with an electronic digital caliper (Farnell, Oberhaching, Germany) two to three times a week over an 83-day period. Tumor volume was calculated according to the formula  $1/2 \times \text{length} \times (\text{width})^2$ . Mice were sacrificed when the tumor volume exceeded 1,500 mm<sup>3</sup>. The animal experimental procedures were approved by the responsible animal protection officer at the DKFZ and by the regional council according to the German protection law.

**Nuclear and cytoplasmic fractionation from infected cells.** NB-324K cells ( $5 \times 10^5$ ) were infected with Del H-1PV or wt H-1PV at an MOI of 1 PFU/cell. Neutralizing antibodies (PV1; a rabbit polyclonal antiserum directed against H-1PV capsids) were added at 2 h postinfection at a dilution of 1/400 to the cell culture medium in order to prevent secondary infections. At 16, 20, and 24 h after infection, cells were harvested and a nucleocytoplasmic fractionation was performed using an NE-PER nuclear and cytoplasmic extraction reagents kit (Thermo Fisher Scientific, Rockford, IL) according to the manufacturer's instructions. The number of infectious particles present in each fraction was determined by plaque assay and expressed as the total number of PFU.

**Immunoblotting.** 293T cells ( $2 \times 10^6$ ) were transfected with 6  $\mu$ g of pDelH1 or pH1 DNA. Cells were harvested at 24 and 48 h posttransfection and lysed in RIPA buffer (150 mM NaCl, 10 mM Tris, pH 7.5, 1 mM EDTA, pH 8.0, 1% [vol/vol] NP-40, 0.5% sodium deoxycholate, 0.1% [wt/vol] sodium dodecyl sulfate [SDS]) supplemented with protease inhibitors (Roche, Germany). After protein quantification (Bio-Rad protein assay; Bio-Rad Laboratories, Munich, Germany), 10  $\mu$ g or 20  $\mu$ g of total proteins (for VP and NS protein analyses, respectively) was separated by SDS–12% polyacrylamide gel electrophoresis (PAGE) and electrotransferred to Protran nitrocellulose membranes (PerkinElmer Life Sciences, Germany). The membranes were incubated with rabbit polyclonal antisera directed against either MVMP NS1 (SP8 [7]) or MVMP NS2 (-NS2p [51]) carboxy-terminal regions or H-1PV capsid proteins ( $\alpha$ -VP [24]) and with appropriate secondary horseradish peroxidase-coupled antibodies (Promega, Mannheim, Germany). Immunoreactive proteins were then revealed by enhanced chemiluminescence (GE Healthcare Europe, Freiburg, Germany).

**Pulse-chase metabolic radiolabeling and cell extracts.** NB-324K cells ( $9 \times 10^5$ ) were infected with either Del H-1PV or wt H-1PV at an MOI of 10 PFU/cell or mock treated (i.e., buffer treated). At 18 h postinfection, cultures were metabolically labeled for 30 min with 200  $\mu$ Ci of Tran<sup>35</sup>S-Label (1,175 Ci/mmol; MP Biomedicals) in Met- and Cys-free DMEM (Sigma) supplemented with 5% dialyzed fetal calf serum, 1% L-glutamine, and 1% gentamicin. Cells were then washed with MEM and either subsequently lysed (chase time, 0 min) or further incubated at 37°C with 5% CO<sub>2</sub> in complete MEM and lysed at various time points of chase in order to investigate the stability of labeled, neosynthesized proteins. Cell lysis was performed using RIPA buffer supplemented with a mixture of proteinase inhibitors (Complete; Roche, Mannheim, Germany). Proteins were harvested after removing cell debris by centrifugation for 10 min at 12,000 rpm and 4°C (centrifuge 5417R; Eppendorf).

**Coimmunoprecipitation assays.** Infected cells were metabolically radiolabeled with Tran<sup>35</sup>S-Label (1,175 Ci/mmol; MP Biomedicals, Irvine, CA) as described above, except for 2 h, before being harvested and lysed in RIPA buffer containing or not containing SDS. After clearing centrifugation of the protein extracts and quantification of incorporated radioactivity in each sample by means of a liquid scintillation analyzer (A1600; PerkinElmer),  $5 \times 10^6$  cpm of radiolabeled protein extracts was first incubated at 4°C for 1 h under continuous rotation (Reax 2; Heidolph) with 8 to 10  $\mu$ l of polyclonal rabbit antisera directed against either NS1 (SP8 [7]) or NS2 ( $\alpha$ -NS2p [51]) or with polyclonal goat antibodies directed against the cellular protein CRM1 (SC-7825; Santa Cruz Biotechnology). The samples were further incubated for 1 h at 4°C in the presence of 100  $\mu$ l of protein A-Sepharose beads (6MB; GE Healthcare) before being pelleted by centrifugation for 5 min at 5,500 rpm and 4°C (centrifuge 2K15; Sigma). Protein-antibody-bead complexes were then washed three times in RIPA buffer (with or without SDS). Complexes were suspended in an appropriate volume of 2 $\times$  SDS-loading dye solution, and immunoprecipitated proteins were separated by 12% SDS-PAGE. After 30 min incubation in Amplify solution (Amersham), gels were dried and exposed to autoradiographic films (BioMax MS films; Kodak).

**Analysis of free and cell-bound virus.** Human NB-324K cells ( $5 \times 10^5$ ) were infected at 4°C with wt H-1PV or Del H-1PV at an MOI of  $10^4$  vg/cell. Cells were harvested by scraping and pelleted by centrifugation for 5 min at 3,500 rpm and 4°C (centrifuge 5417R; Eppendorf), and both supernatants and cell pellets were saved. Cells were suspended in 200  $\mu$ l of ice-cold phosphate-buffered saline (PBS) and lysed, whereas supernatants were incubated at 85°C for 30 min (HBT 130; Haep Labor Consult) in order to denature the viral particles. Recovery of viral DNA from both cell lysates and supernatant fractions was performed using a DNeasy blood and tissue kit (Qiagen) according to the manufacturer's instructions. Quantification of the viral genomes either present in the supernatant fraction or bound to the cells was performed by quantitative real-time PCR (qPCR) as described below.

**Virus uptake.** NB-324K cells ( $8 \times 10^4$ ) were infected with wt H-1PV or Del H-1PV at an MOI of  $10^4$  vg/cell and further incubated at 37°C and 5% CO<sub>2</sub>. At various times of infection (ranging from 0.5 h to 2.5 h), cells were washed with PBS and membrane-bound particles were removed by 5 min treatment with a 0.25% trypsin–1 mM EDTA solution (Invitrogen). After adding cell culture medium, the cells were collected by centrifugation for 5 min at 3,500 rpm and room temperature (centrifuge 5417R; Eppendorf). Viral genomes were recovered from the cell pellets and quantified by qPCR as described below.

**Quantification of packaged viral DNA (qPCR).** The amount of packaged viral genomes was determined by qPCR assays as previously described (26) using a Mastercycler ep realplex instrument (Eppendorf, Hamburg, Germany). Individual reaction mixtures (20  $\mu$ l) contained 1 $\times$  TaqMan Universal PCR master mix (Applied Biosystems), 0.28  $\mu$ M labeled NS1–TaqMan probe, 0.28  $\mu$ M each forward and reverse primer, and 2.85  $\mu$ l template. Virus yields were expressed as the number of viral genomes per ml of virus suspension and calculated according to the following equation:  $I_Q (1/\text{ml}) \times F_{\text{dilution}}$ .  $I_Q$  denotes the quantified fluorescence intensity of a sample, and  $F_{\text{dilution}}$  corresponds to the dilution factor of the virus suspension (in our reaction assays,  $F_{\text{dilution}}$  was 35,000).

**Southern blot analysis.** Extraction of low-molecular-weight viral DNA from infected or transfected cells was performed by using the DNeasy blood and tissue kit (Qiagen) according to the manufacturer's instructions. Viral DNA replicative forms were separated by 1% agarose gel electrophoresis. After gel denaturation in a 1.5 M NaCl, 0.5 M NaOH solution and neutralization in a 1.5 M NaCl, 0.5 M Tris-HCl, pH 7.2, 1 mM EDTA solution, DNA molecules were transferred onto nitrocellulose membranes (Protran; GE Healthcare) for 15 to 20 h at room temperature by capillary action in the presence of 10 $\times$  SSC (1 $\times$  SSC is 0.15 M NaCl plus 0.015 M sodium citrate) buffer and further linked to the membrane by heat treatment for 2 h at 80°C. Membranes were hybridized at 65°C with a <sup>32</sup>P-labeled DNA fragment specific for NS and exposed to autoradiographic films (BioMax MS film; Kodak) at –80°C.

## RESULTS

**Generation and production of Del H-1PV.** To further analyze the effects of the in-frame deletion in the NS-coding sequence previously identified in the variant H-1 dr virus (23), we generated the pDelH1 infectious molecular clone by deleting 114 nucleotides (nt 2022 to 2135) within the left-hand part of the H-1PV genome (Fig. 1A). This in-frame deletion within the NS-coding sequence of the parvovirus genome should lead to the synthesis of NS1 and NS2 proteins lacking an internal set of 38 amino acids (amino acids 587 to 624 and 96 to 133, respectively). As expected, transfection of pDelH1 in permissive cells resulted in the production of shortened NS1 and NS2 proteins, here referred to as delNS1 and delNS2, as can be deduced from the size of the corresponding bands in immunoblotting using antisera directed against either NS1 or NS2P protein (Fig. 1B). These data are in agreement with those previously obtained by immunoprecipitation upon infection of human cells with the H-1 dr variant (23). Although the deletion also affects the untranslated leader region of the R3 transcripts (Fig. 1A), no difference in the expression of the viral capsid proteins VP1 and VP2 was observed at 24 h posttransfection with the two constructs. However, the accumulation of the VPs generated by pDelH1 strongly increased at 48 h posttransfection, when secondary infection cycles may occur (Fig. 1B). For further studies, both pDelH1 and the parental pH1 molecular clones were transfected into human 293T cells to generate master stocks of Del H-1PV and wt H-1PV, respectively, that were then propagated in the permissive human NB-324K cell line.

**Increased yields of infectious virions after infection with Del H-1PV compared to standard (wild-type) H-1PV.** We first ana-



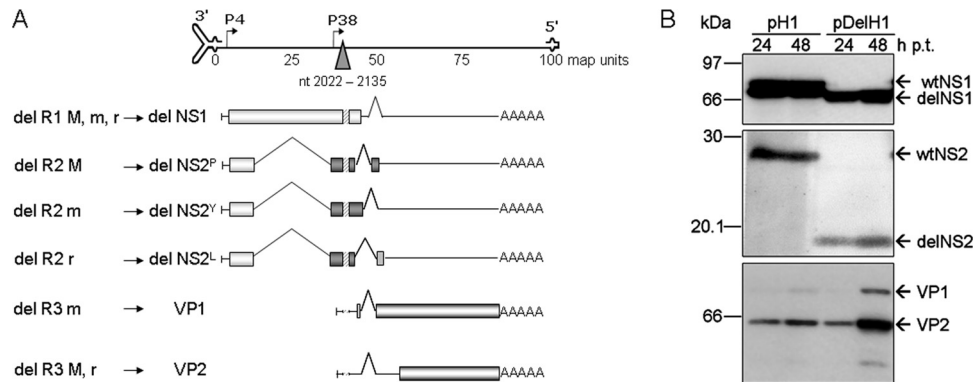


**FIG 1** Schematic representation of Del H-1PV genomic organization and accumulation of the nonstructural delNS1 and delNS2 and capsid VP1 and VP2 proteins. (A) Schematic representation of the viral genome (top) with the 3' and 5' palindromic regions and the P4 and P38 promoters. The triangle indicates the position of the deletion that was introduced in the H-1PV genome. (Bottom) Scheme of the shortened transcripts (lines) and proteins (boxes). The hatched region indicates the localization of the deletion. (B) Accumulation of the nonstructural and capsid proteins expressed from pDelH1 and pH1 in 293T cells. Protein extracts were prepared at 24 h and 48 h posttransfection with either pH1 or pDelH1 and subjected to 12% (NS) or 10% (VP) SDS-PAGE followed by immunoblotting using polyclonal rabbit antisera recognizing either the NS1 protein (top), the NS2P protein (middle), or the VP proteins (bottom).

lyzed the production and infectivity of Del H-1PV compared to those of wt H-1PV. For this, virus stocks were produced in parallel by infection of NB-324K cells and harvested at 3 days postinfection, and the amounts of genome-containing (i.e., full) and plaque-forming (i.e., infectious) particles were determined by quantitative real-time PCR and plaque assay, respectively. The titers of infectious (given in PFU/ml) and full (given in vg/ml) viral particles and the corresponding particle-to-infectivity (P/I) ratios from two independent productions are compiled in Fig. 2A. Although the titers of full particles produced by infection with Del H-1PV and wt H-1PV were quite similar, Del H-1PV yielded higher titers of infectious virions than wt H-1PV, resulting in a significantly (3- to 5-fold) lower P/I ratio with Del H-1PV (Fig. 2A).

The production of Del H-1PV and wt H-1PV infectious virions was also monitored in time course experiments. NB-324K cells were infected with either Del H-1PV or wt H-1PV, and virus particles were recovered at day 1 to 4 postinfection from both the supernatant and cell pellet fractions and quantified by plaque assays. Both viruses gave rise to increasing amounts of infectious progeny virions with time (data not shown). However, the production of infectious particles by Del H-1PV was consistently higher (up to three times) than that by wt H-1PV (Fig. 2B), which is indicative of the enhanced fitness of the Del H-1PV mutant compared with that exhibited by wt H-1PV.

**Enhanced spreading of Del H-1PV compared to wild-type H-1PV.** The increased infectivity of Del H-1PV over wild-type H-1PV virions led us to compare these two viruses for their spread efficiency in cell culture. For that purpose, plaque assays were performed on NB-324K cells, and both the size and occurrence frequency of the plaques produced by Del H-1PV and wt H-1PV were assessed using the image-processing software ImageJ. Both viruses gave rise to a mixture of small and large plaques (Fig. 3A). The occurrence frequency of the various plaque sizes produced by each virus was determined and expressed as the percentage of the total number of analyzed plaques. As shown in Fig. 3B, infection with Del H-1PV gave rise to a higher frequency of large plaques, whereas a higher frequency of small plaques was obtained with wt

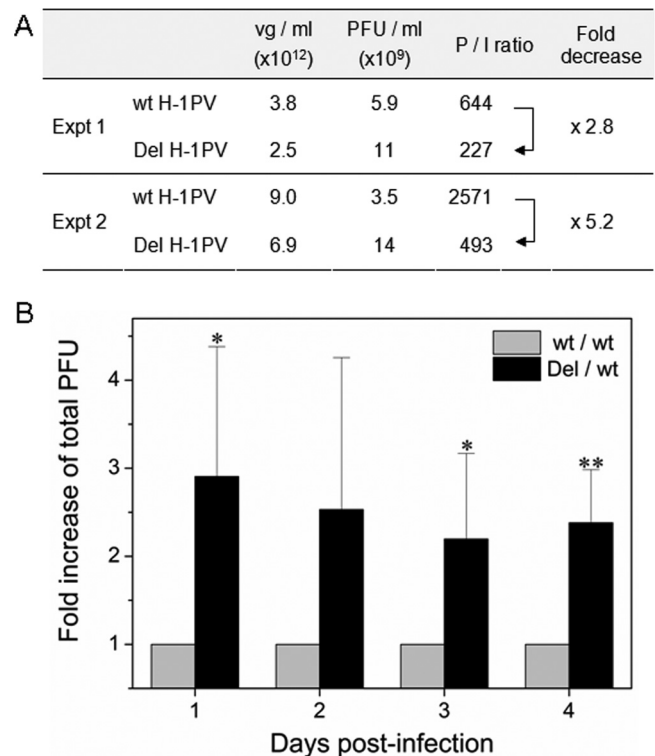


**FIG 2** Del H-1PV progeny production and infectivity are increased in permissive human NB-324K cells. (A) Increased infectivity of Del H-1PV versus wt H-1PV particles. Cells infected with Del H-1PV or wt H-1PV (MOI, 0.003 PFU) were harvested at day 3 p.i. Titers of infectious and full particles were determined by plaque assay (given in PFU/ml) and qPCR (given in vg/ml), respectively. The particle-to-infectivity (P/I) ratio and the fold decrease of the P/I ratio between wt H-1PV and Del H-1PV are indicated. (B) Time course production of Del H-1PV and wt H-1PV. Cells were infected at an MOI of 0.5 PFU. The amounts of infectious virus were determined by plaque assay (infectious particles from both cell extract and culture medium; total PFU). Data are shown as fold increase of Del H-1PV progeny production over wt H-1PV progeny production and represent the means of three independent experiments with the standard deviation (SD). \*,  $P < 0.05$ ; \*\*,  $P < 0.01$ .

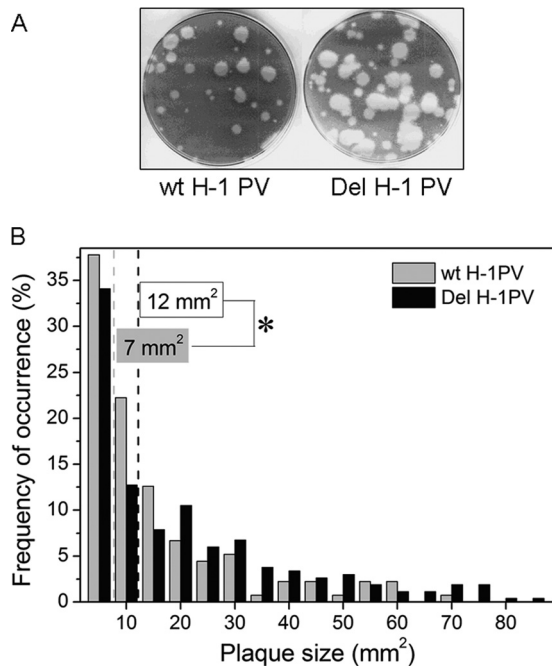


**FIG 3** Enhanced propagation of Del H-1PV compared to wild-type H-1PV in infected NB-324K cells. (A) Illustration of plaque sizes produced by wt H-1PV and Del H-1PV after infection of NB-324K cells. (B) Plaque analysis using the Java-based image-processing software ImageJ. Plaque sizes are given in mm<sup>2</sup>, and frequencies of occurrence are expressed as a percentage of the total number of analyzed plaques:  $n = 135$  for wt H-1PV and  $n = 267$  for Del H-1PV. The means of the plaque sizes produced by wt H-1PV or Del H-1PV are indicated with dotted gray and black lines, with their values given in gray and black boxes, respectively. \*,  $P < 0.05$ .

H-1PV, with the median size of the plaques being 12 mm<sup>2</sup> for the former one and 7 mm<sup>2</sup> for the latter one.

This elevated occurrence of large plaques generated by Del H-1PV indicates a more efficient propagation of the deletion mutant than the wild-type virus, which likely results from the stimulation of some steps of the viral life cycle.

**Enhanced capacity of Del H-1PV for suppressing tumor growth.** NB-324K cells are human cells transformed with the simian virus SV40 (49). In order to rule out the possibility that increased accumulation of Del H-1PV infectious particles might be assigned to helper functions provided by SV40 antigen-expressing cells, the production of Del H-1PV and wt H-1PV was also assayed in different human tumor cell lines. For this, cells of the cervix carcinoma cell line HeLa and two pancreatic ductal adenocarcinoma (PDAC) cell lines, Panc-1 and MiaPaCa-2, were infected at a low MOI (0.5 PFU/cell) with wt H-1PV or Del H-1PV, and virus particles were recovered at various days postinfection and quantified by plaque assays. Maximum yields of infectious virions were obtained at days 3, 5, and 7 upon infection of NB-324K, HeLa, and PDAC cells, respectively. As shown in Fig. 4A, the amount of total (cell-bound and released) infectious particles was higher in the four cell lines upon infection with Del H-1PV than wild-type H-1PV, showing that the improved fitness of Del H-1PV was not restricted to SV40-transformed cell lines or to the tissue origin of the cells. It is worth noting that no detectable production of Del H-1PV progeny virions was observed in human tumor cells known to be sensitive to the wild-type H-1PV-induced killing but

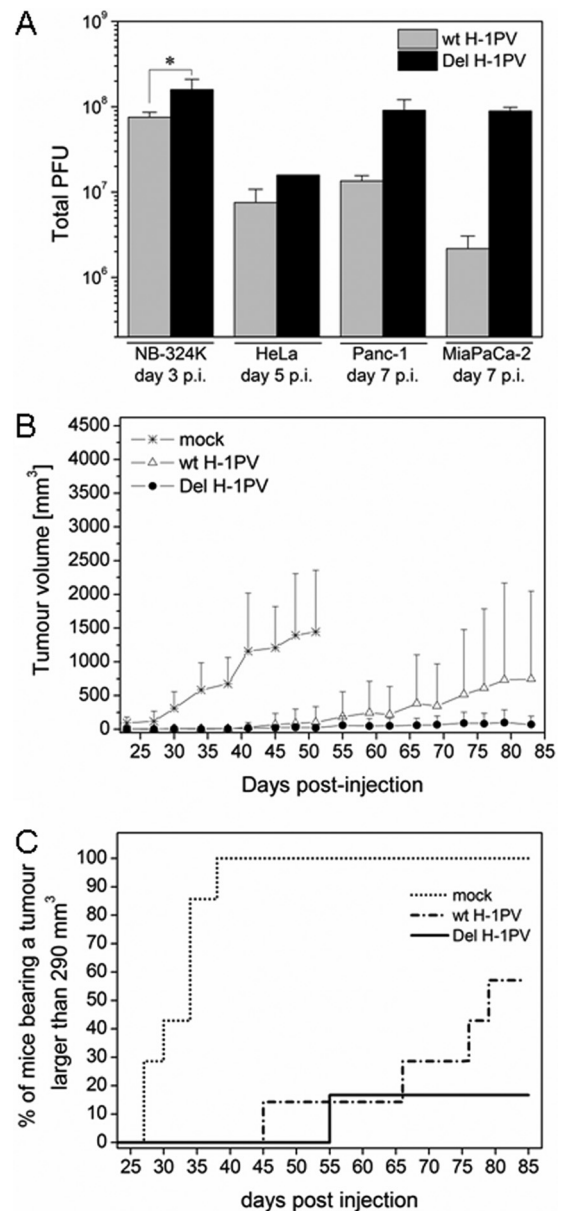


**FIG 4** Del H-1PV production and ability for tumor suppression are more efficient than those for wt H-1PV. (A) Del H-1PV progeny production is increased in various human cell lines. Infectious progeny production of Del H-1PV and wt H-1PV was measured after infection (MOI, 0.5 PFU/cell) of human NB-324K, HeLa, and PDAC Panc-1 and MiaPaCa-2 cell lines. The yields of infectious particles (total numbers of PFU) recovered from both cell supernatants and pellets were determined by plaque assay at days 3, 5, and 7 p.i. for NB-324K, HeLa, and both PDAC cell lines, respectively. \*,  $P < 0.05$ . (B and C) Del H-1PV is more efficient in suppressing the growth of Panc-1 cell-derived tumors than wt H-1PV. Panc-1 cells ( $5 \times 10^6$ ) were buffer treated (mock) or infected with wt H-1PV or Del H-1PV at an MOI of 1 RU/cell and subcutaneously implanted into the right flank of BALB/c nude mice. Tumor appearance and development were monitored over time. (B) Tumor volumes are given as means for 6 or 7 mice/group ( $\pm$  SD); (C) the percentage of mice bearing a tumor larger than 290 mm<sup>3</sup> is plotted as a function of time postimplantation.

resistant to the production of progeny viruses (data not shown), indicating that Del H-1PV cannot bypass this cellular barrier(s) of the parvovirus cycle.

The increased yields of infectious Del H-1PV progeny virions

in permissive human tumor cells prompted us to investigate the efficiency of this deletion mutant in suppressing tumor formation after *ex vivo* infection. To this end, Panc-1 cells were infected at an MOI of 1 RU/cell with either Del H-1PV or wt H-1PV and injected subcutaneously in the right flank of BALB/c nude mice. A control group was inoculated with mock-treated (i.e., buffer-treated) cells. Tumor growth was monitored over an 83-day period post-implantation. As shown in Fig. 4B, mice grafted with mock-treated Panc-1 cells developed tumors from day 30 postimplantation, while tumor appearance was significantly delayed (i.e., up to 15 days) and tumor growth was drastically reduced in mice grafted with cells infected with either wild-type or Del H-1PV. Interestingly, a stronger inhibition of tumor growth was observed in the group of animals that received cells treated with Del H-1PV. This was notably reflected by a further 10-day delay in tumor development in this group, compared with the group that was grafted with wt virus-treated cells, and the lower number of mice (one out of six) which developed a tumor larger than 290 mm<sup>3</sup>. In contrast, in the group that received wild-type H-1PV-infected cells, more than 50% of the animals (i.e., four out of seven) developed tumors larger than 290 mm<sup>3</sup> within the time course of the experiment (Fig. 4C).

Altogether, our data show that Del H-1PV exhibited a stronger capacity than wild-type H-1PV to suppress the growth of human tumor xenografts.

**Increased nuclear export of Del H-1PV progeny virions.** In order to unravel the steps of the PV replication cycle responsible for the enhanced infectivity of Del H-1PV over wt H-1PV, the nuclear release of progeny virions was first investigated in producer cells. Indeed, the main steps of the parvoviral replication cycle take place in the nucleus of infected cells, including genome amplification, capsid assembly, and packaging of single-stranded genome into viral particles (15, 44). Full virions then move out of the nuclear compartment to the cytoplasm, are transported within vesicles to the plasma membrane, and are further released in the cell culture medium (1, 21, 34). Therefore, we determined the nuclear-cytoplasmic distribution of viral particles produced after infection of NB-324K cells in the presence of neutralizing antibodies in order to avoid secondary infections. At 16 h, 20 h, and 24 h postinfection, virions were isolated from both the nucleus and cytoplasm and titrated by plaque assays. The quality of the fractionation procedure was verified by immunoblotting analysis for the presence in nuclear and cytoplasmic protein extracts of the markers lamin B and alpha-tubulin, respectively (data not shown). Significant amounts of infectious particles were retrieved from both the cytoplasmic and nuclear fractions of NB-324K cells upon infection with either Del H-1PV or wt H-1PV at each time point tested (Fig. 5A). In agreement with the above-described results, larger amounts of total (nuclear and cytoplasmic) infectious particles were systematically recovered with Del H-1PV. Furthermore, the deletion mutant and wild-type viruses showed a striking difference in the intracellular distribution of infectious virions. This was most obvious at 24 h p.i., when the amount of infectious particles was 10 times higher in the cytoplasmic fraction of cells infected with Del H-1PV than cells infected with wt H-1PV, whereas the yield of infectious particles associated with the nuclear fraction was not significantly different between the two viruses (Fig. 5A). Accordingly, the ratio of cytoplasmic versus nuclear-associated progeny particles was higher, though vari-

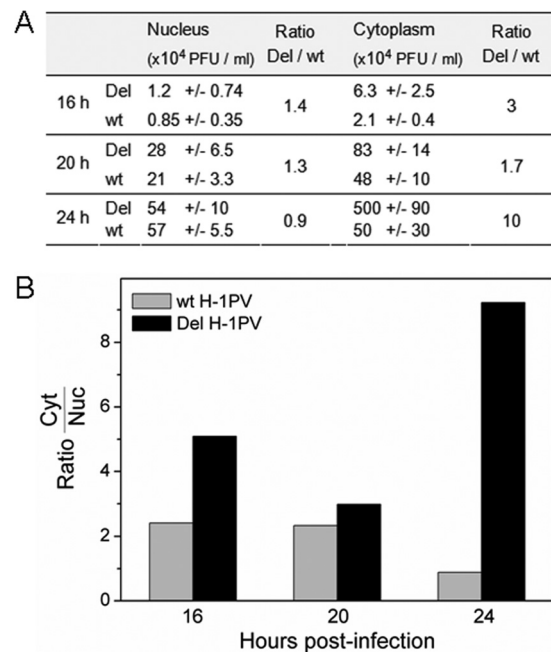


**FIG 5** Earlier nuclear release of Del H-1PV progeny virions in NB-324K cells. NB-324K cells were infected with Del H-1PV or wt H-1PV at an MOI of 1 PFU/cell and further incubated in the presence of neutralizing antibodies. Cells were harvested at the indicated points of time p.i. and subjected to a nuclear-cytoplasmic fractionation. Infectious virus particles present in both fractions were titrated by plaque assay. (A) Titers (in PFU/ml  $\pm$  SD) and ratio of Del H-1PV to wt H-1PV infectious particles are given for nuclear and cytoplasmic fractions. (B) Virus distribution between cytoplasmic (Cyt) and nuclear (Nuc) fractions (cytoplasmic fraction/nuclear fraction ratio) of Del H-1PV and wt H-1PV.

able, upon infection with Del H-1PV at every time point tested (Fig. 5B).

Altogether, these data showed that the increased infectivity of Del H-1PV virions correlated with a change in a, presumably, maturation step in their production, resulting in their more efficient export from the nucleus of infected cells.

**Improved uptake of Del H-1PV virions.** We next determined whether the maturation and/or other genuine properties of Del H-1PV made the mutant virus more competent for distinct steps of the PV replication cycle. First of all, the binding and internalization of wt and Del H-1PV particles were compared in permissive human NB-324K cells. Binding was measured by incubating the cells with Del H-1PV or wild-type H-1PV at 4°C to prevent virus entry and quantifying the genomes of bound full particles by qPCR. Interestingly, the fraction of inoculated Del H-1PV full particles bound to the cells was about 10-fold higher than the one obtained with wt H-1PV (Fig. 6A). The internalization of viral particles was determined by qPCR detection of intracellular viral genomes at various times of infection (0.5 h to 2.5 h) after treatment of virus-infected cells with trypsin-EDTA to remove plasma membrane-bound virions. As shown in Fig. 6B, about 9-fold larger amounts of viral genomes were recovered from lysed cells upon infection with Del H-1PV than upon infection with wt H-1PV, an effect that was detectable at as early as 30 min of infection. Thus, our data showed a striking correlation between the levels of internalized Del H-1PV particles and their higher binding efficiency compared with the results for wt H-1PV. The uncoating

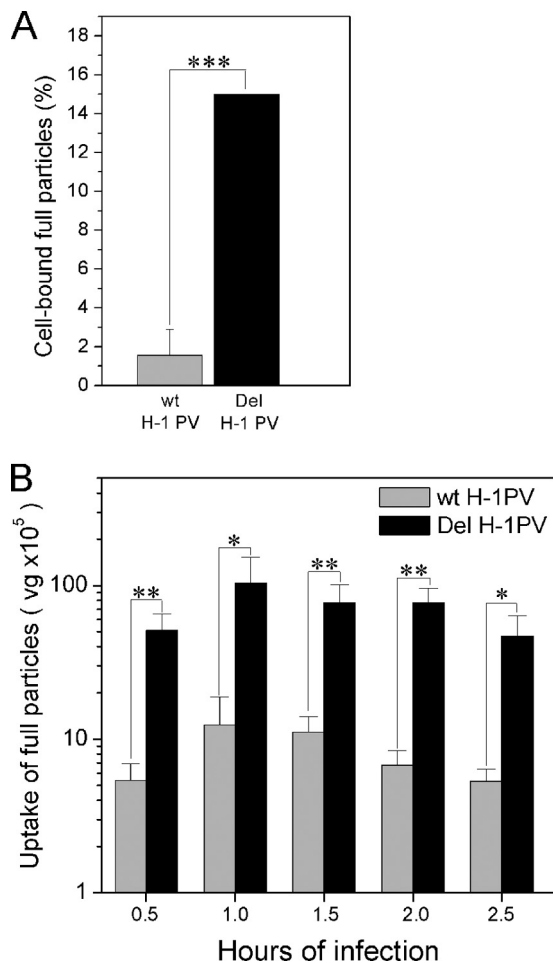


**FIG 6** Improved cell binding (A) and uptake (B) of Del H-1PV particles compared with wt H-1PV particles. (A) NB-324K cells were infected with either wt H-1PV or Del H-1PV at an MOI of  $10^4$  vg/cell and 4°C for 1 h. The amount of cell-bound full particles was determined by qPCR and expressed as the percentage of input viral genome. \*\*\*,  $P < 0.001$ . (B) NB-324K cells were infected at an MOI of  $10^4$  vg/cell and 37°C. Cells were recovered at the indicated times of infection and treated with trypsin-EDTA to remove cell-bound particles. Following cell lysis, the amount of internalized full particles was determined by qPCR and given in vg. \*,  $P < 0.05$ ; \*\*,  $P < 0.01$ .

proneness of Del H-1PV and wt H-1PV was also compared. For that purpose, a cell-free assay was used in which a suspension of viral particles was exposed to gradient temperatures (ranging from 50°C to 70°C) in order to mimic the decapsidation process (13, 46). This showed that Del H-1PV particles were more sensitive to heat denaturation than wt H-1PV particles and raised the possibility that the mutant virus was also more susceptible to uncoating during infection (data not shown).

**Enhanced accumulation of Del H-1PV DNA replicative forms after infection—but not after transfection—of NB-324K cells.** Enhanced uptake and opening up of Del H-1PV particles were expected to result in the stimulation of the viral life cycle. This was confirmed by measuring the accumulation of viral DNA replicative forms in NB-324K cells infected with Del H-1PV or wt H-1PV in the presence of neutralizing antibodies to prevent secondary infection cycles. Viral DNA molecules were extracted at various times postinfection and subjected to Southern blot anal-

ysis. As shown in Fig. 7A (top), both viruses were able to generate mono- and multimeric DNA replicative forms with time. However, RF molecules accumulated in larger amounts in Del H-1PV-infected cells, as shown by stronger signal intensities at given times postinfection. For instance, a 7-fold (monomeric replicative form [mRF]) to 11-fold (dimeric replicative form [dRF]) enhancement of Del H-1PV versus wt H-1PV bands was observed at 9 h p.i. (Fig. 7A, bottom). Accordingly, viral single-stranded DNA (ssDNA), a displacement product derived from RF molecules, became detectable at 12 h p.i. (Fig. 7A, top) at a level that was 19-fold higher in Del H-1PV-infected cells than wt H-1PV-infected cells (Fig. 7A, bottom).

The accumulation of Del H-1PV and wt H-1PV replicative forms was also measured upon transfection of human NB-324K cells with the plasmids pDelH1 and pH1 in the presence of neutralizing antibodies. This experiment was designed to analyze DNA replication of Del H-1PV and wt H-1PV in the absence of any of the earlier steps of the viral life cycle that proved to be enhanced with Del H-1PV (see above) and thereby to determine whether the deletion in the Del H-1PV genome may act in *cis* on viral DNA replication. Viral DNA molecules were extracted at various times posttransfection, subjected to DpnI digestion, and analyzed by Southern blotting assays. In contrast to the data obtained after infection, no significant difference in the appearance and accumulation of viral mRF and dRF molecules was observed between samples transfected with the plasmid pDelH1 and those transfected with pH1 (Fig. 7B). Indeed, mRF and dRF molecules from both Del H-1PV and wt H-1PV were detectable at 16 h p.t., and their amounts increased to similar levels with time, showing that the replication of Del H-1PV DNA *per se* was not stimulated compared to that of wt H-1PV DNA. Altogether, these data indicated that the enhanced fitness of Del H-1PV correlated with the stimulation of both postreplication and prereplication steps of the viral life cycle, i.e., the maturation-dependent egress of virus from the nucleus and the nuclear delivery-dependent onset of virus replication, respectively. Although these events may be stimulated independently, postreplication maturation of virus in primary infected cells may be speculated to play a direct role in the enhanced capacity of Del H-1PV for viral genome delivery to subsequently infected cells.

**Increased turnover of delNS2P proteins: potential role in Del H-1PV fitness?** The shortened nonstructural proteins delNS1 and delNS2 are good candidates for viral effectors involved in the improved fitness of Del H-1PV. Indeed, the in-frame deletion in the Del H-1PV genome results in the alteration of the primary structure of both viral proteins by removing 38 amino acids from their sequences and may thus interfere with their known functioning in the production and intracellular trafficking of progeny virions (1, 21, 38).

It has been previously reported that the NS1 protein of MVMp, a parvovirus closely related to H-1PV, is relatively stable, whereas MVMp NS2 proteins are very labile, with a half-life shorter than 30 min (14, 35). The expression of high levels of MVMp NS2 was also found to be crucial for the parvovirus replication cycle (9, 47). This prompted us to analyze the synthesis and stability of the viral nonstructural proteins expressed from Del H-1PV and wt H-1PV by performing pulse-chase assays. Infected NB-324K cells were pulsed in a [<sup>35</sup>S]methionine/cysteine-containing culture medium for 30 min and harvested either immediately (0 min) or after incubation in nonradioactive medium for various chase periods



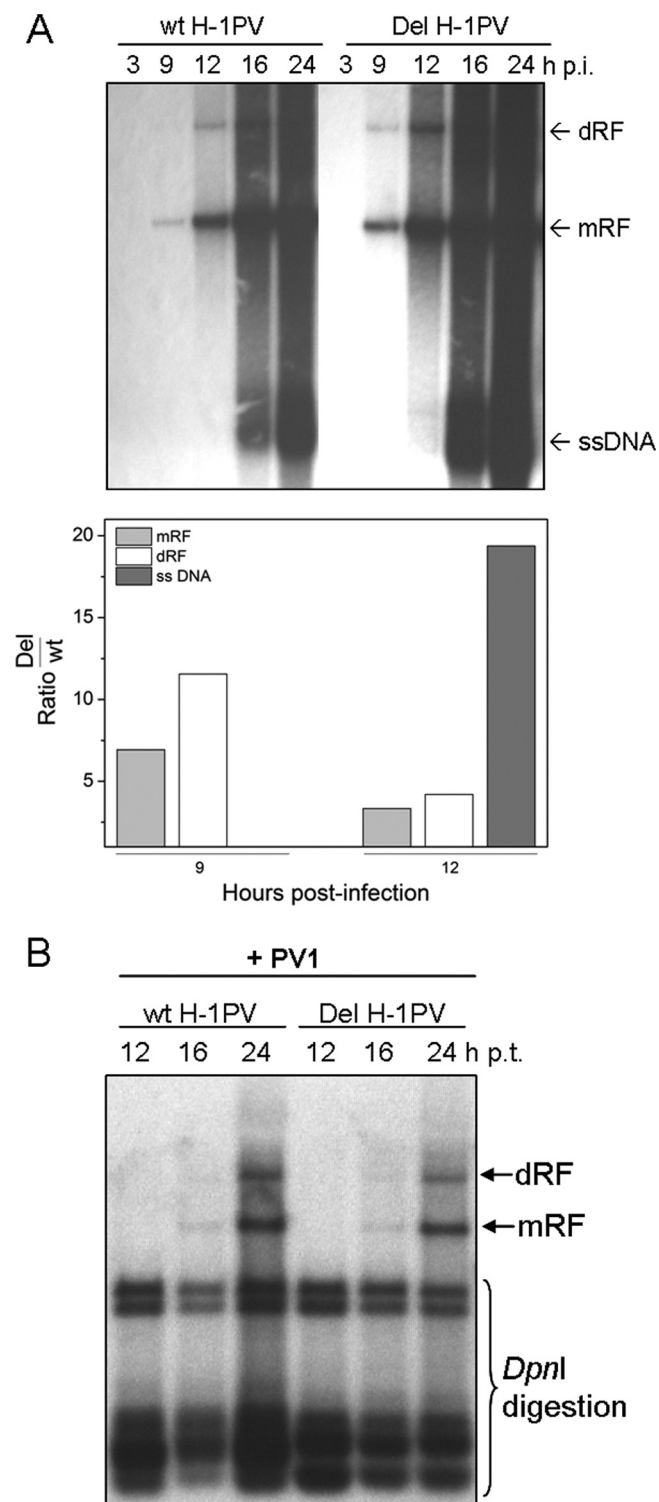


**FIG 7** Increased accumulation of Del H-1PV DNA replicative forms in infected—but not transfected—NB-324K cells. (A) NB-324K cells ( $9 \times 10^5$ ) were infected with wt H-1PV or Del H-1PV at an MOI of 6,844 vg/cell. At 2 h postinfection, neutralizing antibodies were added and cells were harvested at the indicated points of time p.i. Viral DNA replicative forms purified from cell lysates were separated by agarose gel electrophoresis and subjected to Southern blotting. Signal intensities of Del H-1PV and wt H-1PV replicative forms (mRF and dRF) and ssDNA were quantified by PhosphorImager analysis. (Top) Viral replicative intermediates revealed through hybridization with an NS1-specific  $^{32}\text{P}$ -labeled DNA probe; (bottom) ratio of signal intensities cor-

(from 20 min to 240 min). NS1 and NS2 proteins were then immunoprecipitated with appropriate antibodies from the various cell lysates, and the immune complexes were separated by SDS-PAGE and visualized by autoradiography. As shown in Fig. 8, striking differences in the neosynthesis, stability, and/or post-translational modifications of the shortened versus wild-type forms of the viral NS1 and NS2 proteins were observed at 18 h postinfection.

As reported for MVMp NS1 (14), the H-1PV NS1 protein remained stable during the analyzed chase periods (Fig. 8A, top, lanes 1 to 5). This viral protein was first detected as a single band after 30 min of pulse (Fig. 8A, top, lane 1) and appeared as a doublet from 20 min to 40 min of chase, with the retarded band accumulating with time concomitantly with the disappearance of the lower band. The retardation of the slower-migrating NS1 form can likely be assigned to a posttranslational modification(s), in particular, phosphorylation events, as previously described (42). Except for an enhanced rate of neosynthesis and the earlier appearance of modified (retarded) species (Fig. 8A, top, lane 6 versus lane 1), delNS1 was found to be similar to wt NS1 in particular as regards to its high stability (Fig. 8, top, lanes 6 to 11). In contrast to NS1 and as reported for MVMp NS2 (14), wt H-1PV NS2 proved to be more labile, with only small amounts of neosynthesized NS2 still detectable after 240 min of chase (Fig. 8A, bottom, lanes 1 to 5). The synthesis of delNS2P protein was found to be strikingly stimulated in comparison to that of wild-type NS2P (Fig. 8A, bottom, lane 6 versus lane 1), which was much more pronounced than that for NS1 (see above) and is in agreement with a previous report (23). Furthermore, the stability of delNS2P was remarkably reduced, with little neosynthesized protein left after 60 min of chase and no detectable signal after 240 min (Fig. 8A, bottom, lanes 6 to 11). Altogether, our data showed that delNS2 was subject to a higher turnover than wt NS2, which may affect some regulatory function(s) of these viral polypeptides.

We previously reported that MVMp NS2 isoforms interact with the nuclear export factor CRM1 and are actively exported out of the nucleus of infected cells via a CRM1-mediated nuclear export pathway (5). It was also shown that the complex between MVMp NS2 proteins and CRM1 plays a critical role at a late stage of the parvovirus replication cycle, in particular, for the efficient release of progeny virions (21, 22). Therefore, we next wanted to verify the ability of delNS2P (Del H-1PV) and NS2P (wt H-1PV) to form a complex with CRM1. For that purpose, coimmunoprecipitation reactions were performed by using protein extracts from infected NB-324K cells metabolically labeled with [ $^{35}\text{S}$ ] methionine/cysteine and antibodies directed against the nuclear export factor CRM1. As illustrated in Fig. 8B, both wt NS2P and delNS2P coprecipitated with similar efficiency with CRM1 (Fig. 8B, lanes 3 and 5, respectively). Although equivalent amounts of wt NS2P or delNS2P were present in the extracts irrespective of the extraction buffer used (Fig. 8C), no wt NS2P and delNS2P could be detected in immunoprecipitation when using protein extracts

responding to Del H-1PV replicative forms and ssDNA over those corresponding to wt H-1PV ones. (B) NB-324K cells ( $2 \times 10^6$ ) were transfected with 6  $\mu\text{g}$  of pH1 or pDelH1. Neutralizing antibodies (+ PV1) were added 4 h p.t., and cells were harvested at the indicated points of time p.t. Viral DNA replicative forms purified from cell lysates were DpnI digested and analyzed by Southern blotting.



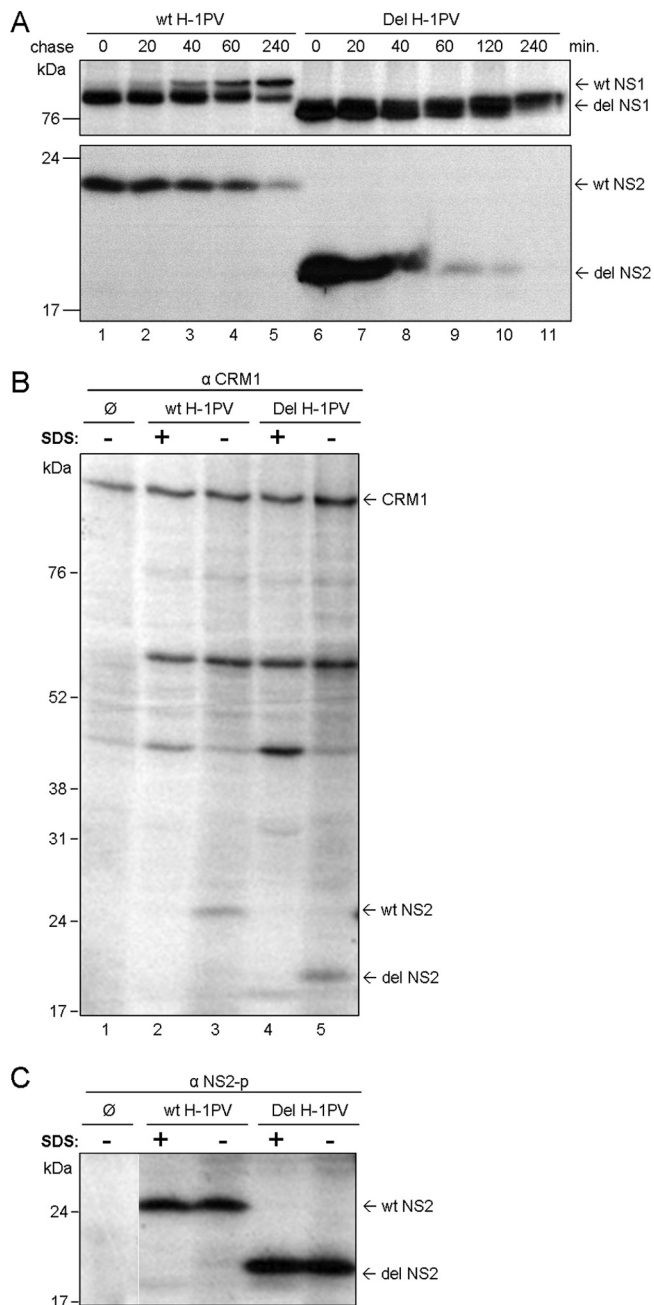


**FIG 8** Increased neosynthesis and degradation of delNS2P compared to wt NS2P protein. (A) Synthesis and stability of delNS2P and wt NS2P in NB-324K cells. Cells were infected with Del H-1PV or wt H-1PV at an MOI of 10 PFU. Proteins were metabolically labeled with [ $^{35}$ S]cysteine/methionine for 30 min (pulse), and cells were further incubated in nonradioactive medium (chase) prior to extraction of the proteins in RIPA buffer at the indicated times. Proteins were immunoprecipitated using rabbit polyclonal antisera recognizing either the NS1 protein (top) or the NS2P protein (bottom), separated by 12% SDS-PAGE, and visualized by autoradiography. (B and C) DelNS2P is able to interact with the nuclear export factor CRM1. Proteins were metabolically labeled with [ $^{35}$ S]cysteine/methionine for 2 h before being extracted in the presence (lanes +) or absence (lanes -) of SDS. Proteins were (co-)immunoprecipitated using rabbit polyclonal antibodies recognizing either CRM1 (B) or NS2P (C), separated by 12% SDS-PAGE, and visualized by autoradiography. The positions of wt NS1 (83 kDa), delNS1 (~76 kDa), wt NS2P (35 kDa), delNS2P (~18 kDa), and CRM1 (110 kDa) are indicated. ∅, mock-treated cells.

obtained in the presence of SDS (Fig. 8B, lanes 2 and 4, respectively), thereby showing the specificity of the reaction. As previously described for MVMp NS2 proteins (7), delNS2P expressed by Del H-1PV was also coprecipitated specifically with members of the 14-3-3 protein family at an efficiency similar to that of H-1PV wt NS2P (data not shown). Altogether, our data indicated that the 38-amino-acid deletion in the delNS2P protein sequence did not impair the ability of the viral protein to interact with its known cellular partners, leaving its possible impact on H-1PV fitness elusive at present.

## DISCUSSION

**Benefit of a deletion in the NS protein-coding sequence for parvovirus fitness.** A naturally occurring, fully infectious variant of H-1PV that has been previously isolated in our laboratory and named H-1 dr was shown to supplant the standard strain in coinfecting human reference cell cultures (23). A large in-frame deletion was identified in the left-hand part of the variant genome; however, the steps of the viral lytic cycle that were affected by this deletion were not investigated. In order to identify the key events in the viral cycle that are involved in the phenotype of this variant, a deletion of nucleotides 2022 to 2135 was introduced in the existing molecular clone of H-1PV, thereby generating the Del H-1PV mutant. The present study showed key benefits of this in-frame, 114-nucleotide-long deletion with regard to the fitness of Del H-1PV. Indeed, the deletion mutant exhibited a better spreading efficacy in cell culture than the wild-type virus. The enhanced fitness correlated with a higher infectivity (decreased full particle-to-infectivity ratio) of the mutant virus but not with an overall increase in the production of full Del H-1PV particles per cell. This argues against a preferential encapsidation of the Del H-1PV genome and suggests that the quality rather than the quantity of the Del H-1PV stocks produced was improved. The enhanced infectivity of Del H-1PV correlated with export of a higher proportion of Del H-1PV progeny virions from the nucleus to the cytoplasm, followed by an overall stimulation of the viral replicative cycle in subsequent infections. In comparison with wt H-1PV, Del H-1PV indeed showed a higher capacity for cell binding, internalization, and presumably also decapsidation of the viral genome.

The above-described large deletion in the NS gene showed key benefits in human cells with respect to wild-type H-1PV. It is worth mentioning that, besides the naturally occurring H-1 dr variant (23), glioma-adapted H-1PV variants selected by passaging in human glioma-derived cell lines were found to harbor a large deletion affecting the left-hand part of their genome (J. P. F. Nüesch, personal communication). Intriguingly, none of the newly described rodent parvoviruses isolated within the past years from laboratory animals exhibited such a deletion in the NS sequence, but various, mostly subtle, changes in the nucleotide sequence of their genome were reported (2–4, 31, 50). This suggests that the emergence of a large deletion within the NS gene may not occur easily during evolution, at least in their natural host. This may be due to NS2 functions that are required for parvovirus replication in host (rodent) cells but dispensable in human cells (12, 28, 29). Supporting this, both H-1 dr and glioma-adapted H-1PV variants failed to replicate efficiently in rat cells, in contrast to wt H-1PV (23).

**Stimulation of Del H-1PV virion maturation.** In MVM it was shown that some modifications of the viral capsids, in particular,

the phosphorylation of specific VP2 amino acids, play an important role in the nuclear maturation of progeny virions (32, 33). The capsomers are assembled in the cytoplasm of virus-infected cells in the forms of VP1/VP2 trimers (44) which are transported into the nucleus for capsid assembly upon phosphorylation via the cell kinase Raf-1 (45). The Raf-1-dependent phosphorylation not only plays a role in the nuclear transport of MVM capsid assembly intermediates but also is required for virus maturation and propagation (45). Indeed, the VP2 amino termini carry phosphoserine-rich export signals, which direct full virions to be trafficked out of the nucleus prior to cell lysis (33). Therefore, the phosphorylation pattern of the capsid proteins encoded by Del H-1PV is worth being investigated. Of note, even if phosphorylation of the capsid proteins appears to be a prerequisite for the nuclear export of progeny virions, one cannot exclude the possibility that other posttranslational events, such as glycosylation or acetylation, may also participate in the maturation of progeny virions.

The deletion in the genome of Del H-1PV results in the expression of NS1 and NS2 proteins that are shortened by 38 amino acids in their C-terminal and internal parts, respectively. This may modify not only the structure but also some specific functions of these proteins. Although little is known about the exact functions of the parvoviral NS2 protein, it was reported to be involved in regulatory activities during viral DNA replication (12, 36), translation of viral mRNA (37), capsid assembly, and nuclear release of progeny virions (12, 21). NS2 proteins were shown to be dispensable for production of progeny virions in non-host cells (12, 21). Nevertheless, they appear to be required for an efficient release of progeny virions out of the productive cells and for the cytotoxic activity of the virus in transformed human cells (6, 12, 21). The molecular mechanism by which truncated NS proteins enhance the nuclear egress of infectious virions is still puzzling. One can hypothesize that NS2 controls some posttranslational modifications of the VP proteins. Indeed, MVMp mutants lacking VP2 amino-terminal phosphorylation were found to form tiny plaques on human indicator cells (32) as a result of an impaired nuclear export of mutant virions from productive cells (33). This phenotype is similar to the one previously described for some MVMp-NS2NES(−) or MVMp-NS2null mutants in human cells (12, 21). Altogether, these data suggest that the viral NS2 proteins contribute to the regulation of some capsid protein posttranslational modifications, in particular, of phosphorylation events leading to an enhanced production of infectious virions. Interestingly, MVM mutants having a few mutations in the second exon of the NS2 proteins proved to exhibit an enhanced cytoplasmic sequestration of CRM1 at the perinuclear membrane together with a larger yield of infectious particles, suggesting that mutated NS2 proteins having a higher affinity for CRM1 may lead to an accelerated virus life cycle and thus to increased fitness (31). The deletion does not affect the nuclear export signal (NES) of NS2 and did not impair its interaction with the cellular proteins CRM1 or members of the 14-3-3 family. However, the binding affinity of delNS2 to its cellular partners, in particular, CRM1, was not analyzed in this study. Comparing the binding affinity of both the H-1PV delNS2 and wild-type NS2 might also help to decipher the molecular mechanisms behind the nuclear release of mature virions.

The above-described large deletion affects not only NS2 but also NS1. The parvoviral NS1 protein is a multifunctional protein essential for viral DNA amplification and gene expression (15).

The fact that Del H-1PV and wt H-1PV stocks were produced at similar titers of full genome-containing particles suggested that the deletion in the NS-coding sequence did not significantly affect the replicative activities of NS1. This was supported by the detection of similar amounts of the DNA replicative forms in cells transfected with either infectious plasmid. NS1 activities were shown to be regulated by posttranslational modifications (16, 42). In particular, phosphorylation events driven by host cellular protein kinases, including protein kinase C  $\lambda$  (PKC $\lambda$ ) (19, 40) and PKC $\eta$  (25), play a key role in the regulation of MVMp NS1 functioning. Present data give a first indication that delNS1 may differ from wt NS1 as regards the timing and possibly also pattern of posttranslational modifications. Whether this difference may affect the process of progeny viral particle maturation through a regulatory cascade is presently a matter of speculation. We are currently testing the working hypothesis that delNS2 and/or delNS1 may be especially efficient in activating specific kinases whose phosphorylated substrates (including the viral capsids?) constitute signals for the nuclear egress of Del H-1PV progeny virions and their maturation to a form prone to uptake in subsequent infections. Altogether, our results point to virion maturation as a highly regulated event determining the overall fitness of rodent parvoviruses and their mutant derivatives.

## ACKNOWLEDGMENTS

We are grateful to S. Paschek and M. Lavie for their kind help in animal experiments and qPCR, respectively, to S. Dempe and J. P. F. Nüesch for critical discussions, and to O. J. Weiss for his assistance in editing the figures.

N.W. was supported by a fellowship from FAZIT Stiftung (Frankfurt am Main, Germany).

## REFERENCES

- Baer S, Daeffler L, Rommelaere J, Nüesch JPF. 2008. Vesicular egress of non-enveloped lytic parvoviruses depends on gelsolin functioning. *PLoS Pathog.* 4:e1000126. doi:10.1371/journal.ppat.1000126.
- Ball-Goodrich LJ, Leland SE, Johnson EA, Paturzo FX, Jacoby RO. 1998. Rat parvovirus type 1: the prototype for a new rodent parvovirus serogroup. *J. Virol.* 72:3289–3299.
- Besselsen DG, et al. 1996. Molecular characterization of newly recognized rodent parvoviruses. *J. Gen. Virol.* 77(Pt 5):899–911.
- Besselsen DG, Romero MJ, Wagner AM, Henderson KS, Livingston RS. 2006. Identification of novel murine parvovirus strains by epidemiological analysis of naturally infected mice. *J. Gen. Virol.* 87:1543–1556.
- Bodendorf U, Cziepluch C, Jauniaux J-C, Rommelaere J, Salome N. 1999. Nuclear export factor CRM1 interacts with nonstructural proteins NS2 from parvovirus minute virus of mice. *J. Virol.* 73:7769–7779.
- Brandenburger A, Legendre D, Avalosse B, Rommelaere J. 1990. NS-1 and NS-2 proteins may act synergistically in the cytopathogenicity of parvovirus MVMp. *Virology* 174:576–584.
- Brockhaus K, Plaza S, Pintel D, Rommelaere J, Salome N. 1996. Non-structural proteins NS2 of minute virus of mice associate in vivo with 14-3-3 protein family members. *J. Virol.* 70:7527–7534.
- Brownstein DG, et al. 1992. The pathogenesis of infection with minute virus of mice depends on expression of the small nonstructural protein NS2 and on the genotype of the allotropic determinants VP1 and VP2. *J. Virol.* 66:3118–3124.
- Choi E-Y, Newman AE, Burger L, Pintel D. 2005. Replication of minute virus of mice DNA is critically dependent on accumulated levels of NS2. *J. Virol.* 79:12375–12381.
- Christensen J, Cotmore SF, Tattersall P. 1995. Minute virus of mice transcriptional activator protein NS1 binds directly to the transactivation region of the viral P38 promoter in a strictly ATP-dependent manner. *J. Virol.* 69:5422–5430.
- Clemens KE, Pintel DJ. 1988. The two transcription units of the autonomous parvovirus minute virus of mice are transcribed in a temporal order. *J. Virol.* 62:1448–1451.

12. Cotmore SF, D'Abramo AM, Carbonell LF, Bratton J, Tattersall P. 1997. The NS2 polypeptide of parvovirus MVM is required for capsid assembly in murine cells. *Virology* 231:267–280.
13. Cotmore SF, D'Abramo AM, Ticknor CM, Tattersall P. 1999. Controlled conformational transitions in the MVM virion expose the VP1 N-terminus and viral genome without particle disassembly. *Virology* 254: 169–181.
14. Cotmore SF, Tattersall P. 1990. Alternate splicing in a parvoviral non-structural gene links a common amino-terminal sequence to downstream domains which confer radically different localization and turnover characteristics. *Virology* 177:477–487.
15. Cotmore SF, Tattersall P. 1995. DNA replication in the autonomous parvoviruses. *Semin. Virol.* 6:271–281.
16. Cotmore SF, Tattersall P. 1986. The NS-1 polypeptide of the autonomous parvovirus MVM is a nuclear phosphoprotein. *Virus Res.* 4:243–250.
17. Cotmore SF, Tattersall P. 2007. Parvoviral host range and cell entry mechanisms. *Adv. Virus Res.* 70:183–232.
18. Dempe S, Stroh-Dege AY, Schwarz E, Rommelaere J, Dinsart C. 2010. SMAD4: a predictive marker of PDAC cell permissiveness for oncolytic infection with parvovirus H-1PV. *Int. J. Cancer* 126:2914–2927.
19. Dettwiler S, Rommelaere J, Nuesch JPF. 1999. DNA unwinding functions of minute virus of mice NS1 protein are modulated specifically by the lambda isoform of protein kinase C. *J. Virol.* 73:7410–7420.
20. Doerig C, Hirt B, Beard P, Antonietti J-P. 1988. Minute virus of mice non-structural protein NS-1 is necessary and sufficient for trans-activation of the viral P39 promoter. *J. Gen. Virol.* 69:2563–2573.
21. Eichwald V, Daeflter L, Klein M, Rommelaere J, Salome N. 2002. The NS2 proteins of parvovirus minute virus of mice are required for efficient nuclear egress of progeny virions in mouse cells. *J. Virol.* 76:10307–10319.
22. Engelsma D, et al. 2008. A supraphysiological nuclear export signal is required for parvovirus nuclear export. *Mol. Biol. Cell* 19:2544–2552.
23. Faisst S, et al. 1995. Isolation of a fully infectious variant of parvovirus H-1 supplanting the standard strain in human cells. *J. Virol.* 69:4538–4543.
24. Kestler J, et al. 1999. Cis requirements for the efficient production of recombinant DNA vectors based on autonomous parvoviruses. *Hum. Gene Ther.* 10:1619–1632.
25. Lachmann S, Rommelaere J, Nuesch JPF. 2003. Novel PKCeta is required to activate replicative functions of the major nonstructural protein NS1 of minute virus of mice. *J. Virol.* 77:8048–8060.
26. Lacroix J, et al. 2010. Parvovirus H1 selectively induces cytotoxic effects on human neuroblastoma cells. *Int. J. Cancer* 127:1230–1239.
27. Lang SI, et al. 2005. The infectivity and lytic activity of minute virus of mice wild-type and derived vector particles are strikingly different. *J. Virol.* 79:289–298.
28. Li X, Rhode SL III. 1991. Nonstructural protein NS2 of parvovirus H-1 is required for efficient viral protein synthesis and virus production in rat cells in vivo and in vitro. *Virology* 184:117–130.
29. Li X, Rhode SL III. 1993. The parvovirus H-1 NS2 protein affects viral gene expression through sequences in the 3' untranslated region. *Virology* 194:10–19.
30. Li X, Rhode SL III. 1990. Mutation of lysine 405 to serine in the parvovirus H-1 NS1 abolishes its functions for viral DNA replication, late promoter trans activation, and cytotoxicity. *J. Virol.* 64:4654–4660.
31. Lopez-Bueno A, Villarreal LP, Almendral JM. 2006. Parvovirus variation for disease: a difference with RNA viruses? *Curr. Top. Microbiol. Immunol.* 299:349–370.
32. Maroto B, Ramirez JC, Almendral JM. 2000. Phosphorylation status of the parvovirus minute virus of mice particle: mapping and biological relevance of the major phosphorylation sites. *J. Virol.* 74:10892–10902.
33. Maroto B, Valle N, Saffrich R, Almendral JM. 2004. Nuclear export of the nonenveloped parvovirus virion is directed by an unordered protein signal exposed on the capsid surface. *J. Virol.* 78:10685–10694.
34. Miller CL, Pintel DJ. 2002. Interaction between parvovirus NS2 protein and nuclear export factor Crm1 is important for viral egress from the nucleus of murine cells. *J. Virol.* 76:3257–3266.
35. Miller CL, Pintel DJ. 2001. The NS2 protein generated by the parvovirus minute virus of mice is degraded by the proteasome in a manner independent of ubiquitin chain elongation or activation. *Virology* 285:346–355.
36. Naeger LK, Cater J, Pintel DJ. 1990. The small nonstructural protein (NS2) of the parvovirus minute virus of mice is required for efficient DNA replication and infectious virus production in a cell-type-specific manner. *J. Virol.* 64:6166–6175.
37. Naeger LK, Salome N, Pintel DJ. 1993. NS2 is required for efficient translation of viral mRNA in minute virus of mice-infected murine cells. *J. Virol.* 67:1034–1043.
38. Nuesch JPF, Bär S, Lachmann S, Rommelaere J. 2009. Ezrin-radixin-moesin family proteins are involved in parvovirus replication and spreading. *J. Virol.* 83:5854–5863.
39. Nuesch JPF, Bär S, Rommelaere J. 2008. Viral proteins killing tumor cells: new weapons in the fight against cancer. *Cancer Biol. Ther.* 7:1374–1376.
40. Nuesch JPF, Lachmann S, Corbau R, Rommelaere J. 2003. Regulation of minute virus of mice NS1 replicative functions by atypical PKC lambda in vivo. *J. Virol.* 77:433–442.
41. Ohshima T, et al. 1999. CRM1 mediates nuclear export of nonstructural protein 2 from parvovirus minute virus of mice. *Biochem. Biophys. Res. Commun.* 264:144–150.
42. Paradiso PR. 1984. Identification of multiple forms of the noncapsid parvovirus protein NCVP1 in H-1 parvovirus-infected cells. *J. Virol.* 52: 82–87.
43. Pear WS, Nolan GP, Scott ML, Baltimore D. 1993. Production of high-titer helper-free retroviruses by transient transfection. *Proc. Natl. Acad. Sci. U. S. A.* 90:8392–8396.
44. Riobobos L, Reguera J, Mateu MG, Almendral JM. 2006. Nuclear transport of trimeric assembly intermediates exerts a morphogenetic control on the icosahedral parvovirus capsid. *J. Mol. Biol.* 357:1026–1038.
45. Riobobos L, et al. 2010. Viral oncolysis that targets Raf-1 signaling control of nuclear transport. *J. Virol.* 84:2090–2099.
46. Ros C, Baltzer C, Mani B, Kempf C. 2006. Parvovirus uncoating in vitro reveals a mechanism of DNA release without capsid disassembly and striking differences in encapsidated DNA stability. *Virology* 345:137–147.
47. Ruiz Z, D'Abramo A, Jr, Tattersall P. 2006. Differential roles for the C-terminal hexapeptide domains of NS2 splice variants during MVM infection of murine cells. *Virology* 349:382–395.
48. Schoborg RV, Pintel DJ. 1991. Accumulation of MVM gene products is differentially regulated by transcription initiation, RNA processing and protein stability. *Virology* 181:22–34.
49. Tattersall P, Bratton J. 1983. Reciprocal productive and restrictive virus-cell interactions of immunosuppressive and prototype strains of minute virus of mice. *J. Virol.* 46:944–955.
50. Wan CH, Soderlund-Venermo M, Pintel DJ, Riley LK. 2002. Molecular characterization of three newly recognized rat parvoviruses. *J. Gen. Virol.* 83:2075–2083.
51. Wrzesinski C, et al. 2003. Chimeric and pseudotyped parvoviruses minimize the contamination of recombinant stocks with replication-competent viruses and identify a DNA sequence that restricts parvovirus H-1 in mouse cells. *J. Virol.* 77:3851–3858.
52. Young PJ, Jensen KT, Burger LR, Pintel DJ, Lorson CL. 2002. Minute virus of mice small nonstructural protein NS2 interacts and colocalizes with the Smn protein. *J. Virol.* 76:6364–6369.
53. Young PJ, et al. 2005. Minute virus of mice small non-structural protein NS2 localizes within, but is not required for the formation of, Smn-associated autonomous parvovirus-associated replication bodies. *J. Gen. Virol.* 86:1009–1014.
54. Zadori Z, Szelei J, Tijssen P. 2005. SAT: a late NS protein of porcine parvovirus. *J. Virol.* 79:13129–13138.
55. Zolotukhin S, et al. 1999. Recombinant adeno-associated virus purification using novel methods improves infectious titer and yield. *Gene Ther.* 6:973–985.